

# **LEGIBILITY NOTICE**

A major purpose of the Technical Information Center is to provide the broadest dissemination possible of information contained in DOE's Research and Development Reports to business, industry, the academic community, and federal, state and local governments.

Although a small portion of this report is not reproducible, it is being made available to expedite the availability of information on the research discussed herein.

LA-UR- 90 - 2108

Los Alamos National Laboratory is operated by the University of California for the United States Department of Energy under contract W-7405-ENG-84

LA-UR--90-2108

DE90 013160

TITLE NUCLEAR MEDIUM EFFECTS ON QUARKS, GLUONS, AND ON VECTOR MESON  
PRODUCTION: NEW INSIGHTS FROM DIMUON PRODUCTION

AUTHOR(S) M. J. Leitch, D. Alde, H. Baer, T. Carey, G. T. Garvey, A. Klein,  
C. Lee, J. Lillberg, P. McGaughey, C. S. Mishra, J. M. Moss,  
J. C. Peng, C. N. Brown, W. E. Cooper, Y. B. Hsiung, M. R. Adams,  
R. Guo, D. M. Kaplan, R. L. McCarthy, G. Danner, M. Wang, M.  
Bartlett, and G. Hoffmann.

SUBMITTED TO Invited talk presented at the "Symposium in Honor of Akito Arima:  
Nuclear Physics in the 1990's", held in Santa Fe, New Mexico,  
1-5 May, 1990.

### DISCLAIMER

This report was prepared as an account of work sponsored by an agency of the United States Government. Neither the United States Government nor any agency thereof, nor any of their employees, makes any warranty, express or implied, or assumes any legal liability or responsibility for the accuracy, completeness, or usefulness of any information, apparatus, product, or process disclosed, or represents that its use would not infringe privately owned rights. Reference herein to any specific commercial product, process, or service by trade name, trademark, manufacturer, or otherwise does not necessarily constitute or imply its endorsement, recommendation, or favoring by the United States Government or any agency thereof. The views and opinions of authors expressed herein do not necessarily state or reflect those of the United States Government or any agency thereof.

By acceptance of this article the publisher recognizes that the U.S. Government retains a nonexclusive, royalty-free license to publish or reproduce the published form of this contribution or to allow others to do so for U.S. Government purposes.

The Los Alamos National Laboratory requests that the publisher identify this article as work performed under the auspices of the U.S. Department of Energy.

**Los Alamos** Los Alamos National Laboratory  
Los Alamos, New Mexico 87545

FORM NO. 638-94  
87-NO. 7679-1-01

**MASTER**

NUCLEAR DEPENDENCE OF DIMUON  
AND VECTOR-MESON PRODUCTION AT 800 GEV/C

M. J. Leitch, D. M. Alde, H. W. Baer, T. A. Carey, G. T. Garvey,  
A. Klein, C. Lee, J. W. Lillberg, P. L. McGaughey,  
C. S. Mishra, J. M. Moss, J. C. Peng  
*Los Alamos National Laboratory, Los Alamos, New Mexico 87545*

C. N. Brown, W. E. Cooper, Y. B. Hsiung  
*Fermilab, Batavia, Illinois 60510*

M. R. Adams  
*University of Illinois at Chicago, Chicago, Illinois 60680*

R. Guo, D. M. Kaplan  
*Northern Illinois University, DeKalb, Illinois 60115*

R. L. McCarthy  
*SUNY at Stony Brook, Stony Brook, New York 11794-3800*

G. Danner, M. J. Wang  
*Case Western Reserve University, Cleveland, Ohio 44106*  
and  
*Los Alamos National Laboratory, Los Alamos, New Mexico 87545*  
and

M. L. Barlett, G. W. Hoffmann  
*University of Texas, Austin, Texas 78712*

A precise measurement of the atomic mass dependence of dimuon continuum and vector-meson production induced by 800 GeV/c protons is reported. Approximately 700,000 muon pairs with dimuon mass  $M \geq 3 \text{ GeV}$  were recorded from targets of  $^2\text{H}$ ,  $\text{C}$ ,  $\text{Ca}$ ,  $\text{Fe}$ , and  $\text{W}$ . The dimuon mass spectrum obtained is shown in Fig. 1. The ratio of Drell-Yan dimuon yield per nucleon for nuclei versus  $^2\text{H}$ ,  $R = Y_A/Y_{^2\text{H}}$ , is sensitive to modifications of the antiquark sea in nuclei. No nuclear dependence of this ratio is observed over the range of target-quark momentum fraction  $0.1 < x_t < 0.3$ . For  $x_t < 0.1$  the ratio is slightly less than unity for the heavy nuclei. These results are compared with predictions of models of the EMC effect. A depletion of the yield per nucleon from heavy nuclei is observed for the  $J\psi$ ,  $\psi'$ , and  $\Upsilon$  production. This depletion exhibits strong dependence on  $x_f$  and  $p_t$ .

**Nuclear Medium Effects on Quarks, Gluons, and on Vector Meson  
Production: New Insights from Dimuon Production**

M. J. Leitch\* , D. Alde, H. Baer, T. Carey, G. T. Garvey, A. Klein, C. Lee,  
J. Lillberg, P. McGaughey, C. S. Mishra, J. M. Moss, J. C. Peng  
Los Alamos National Laboratory, Los Alamos, New Mexico 87545

C. N. Brown, W. E. Cooper, Y. B. Hsiung,  
Fermilab, Batavia, Illinois 60510

M. R. Adams,  
University of Illinois at Chicago, Chicago, Illinois 60680

R. Guo, D. M. Kaplan,  
Northern Illinois University, DeKalb, Illinois 60115

R. L. McCarthy,  
SUNY at Stony Brook, Stony Brook, New York 11794-3800

G. Danner, M. Wang,  
Case Western Reserve, Cleveland, Ohio 44106

and

M. Bartlett, G. Hoffmann,  
University of Texas, Austin, Texas 78712

\*Talk presented at the "Symposium in Honor of Akito Arima: Nuclear Physics  
in the 1990's", held in Santa Fe, New Mexico, 1-5 May 1990.

## Introduction

Two of the most important and interesting questions in Nuclear Physics today are: 1) How is the intrinsic structure of the nucleon modified in nuclei, and 2) How are reactions on nuclei affected by processes which involve explicit quark and gluon degrees of freedom? In this talk I will try to address some aspects of these questions. In particular I will first discuss in simple terms some basic ideas about the intrinsic structure of the nucleon and its modification in nuclei. I will also identify some of the reaction dynamics issues that must be considered when trying to understand high-energy reactions on nuclei, in particular proton-induced Drell-Yan and resonance production. I will then introduce our experiment, Fermilab E772, and will show our results on the nuclear mass dependence of Drell-Yan and of resonance production. Finally I will summarize the main conclusions.

### I. Structure Functions and Reaction Dynamics

Three of the main processes used for determining the intrinsic structure of a nucleon are shown in Fig. 1. These are deep-inelastic lepton scattering (DIS) where a muon or electron interacts via a virtual photon with the quarks inside a nucleon. The resulting information on the struck quark is extracted in the form of a structure function which gives the probability for the quark in the nucleon to have a certain fraction,  $x$ , of the nucleon momentum. The Drell-Yan process involves the annihilation of a proton beam quark (anti-quark) with a target anti-quark (quark) producing an energetic  $\gamma$  which then decays into a lepton pair. The DIS process is sensitive to the sum of the quark and anti-quark distributions in the target nucleon while DY, in the kinematic

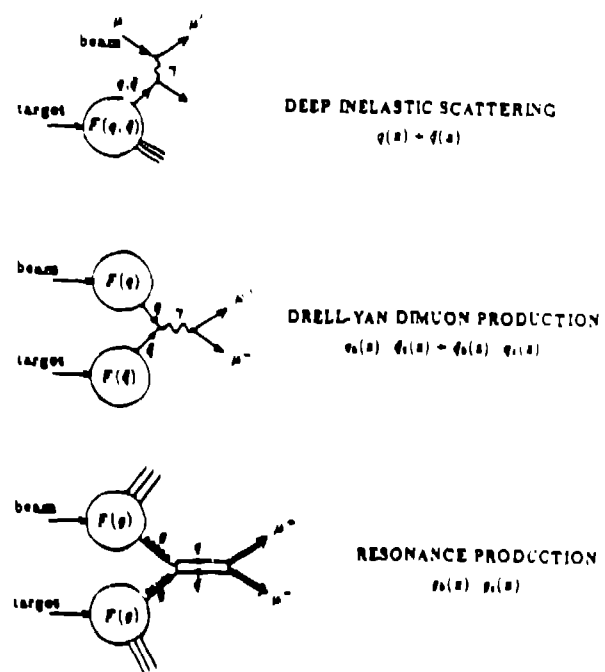


Fig. 1. Processes used for determining nucleon structure functions.

region of our experiment, is primarily sensitive to only that for the target anti-quark. For resonance production ( $J/\psi$ ,  $\psi'$ , and  $\Upsilon$ ) the dominant mechanism is that of gluon-fusion which involves the product of the beam and target gluon structure functions. Nucleon structure functions are shown in Fig. 2.<sup>1</sup> Here we can see that for our Drell-Yan experiment where  $x_1$  (the beam quark momentum fraction) is fairly large we have almost exclusively beam quarks. Thus the annihilation is with a target sea anti-quark and the Drell-Yan measurements determine the target anti-quark structure function in a nucleus.

A number of reaction dynamics effects must be considered when studying these high-energy reactions.<sup>2</sup> Some of these are depicted in cartoon form in Fig. 3. For the Drell-Yan process we expect to see some initial-state multiple scattering effects which will broaden the transverse momentum,  $p_T$ , of the dimuon pair. In the case of resonance production, e.g.  $J/\psi$  production, the situation is more complicated. A  $c\bar{c}$  pair is formed in an almost point-like interaction and then must spread out for a considerable distance (e.g. 5-10 nuclear radii) at which it achieves  $z$  separation distance corresponding to the  $J/\psi$  diameter and it hadronizes. In addition a splash of low-energy  $\pi$ 's and  $\rho$ 's is created by the incident beam quarks. Some of these can be co-moving with the  $J/\psi$ , i.e. have small relative velocity with respect to the  $J/\psi$ . The pre- $J/\psi$  can then be multiple scattered  $\therefore$  can be dissociated by the co-movers. The pre- $J/\psi$  can also be dissociated by the nuclear medium directly, however since the co-movers can continue to interact well outside of the nuclear volume they may in principle have a more important effect.

Data for the A-dependence of the structure function from DIS for both muons (EMC)<sup>3</sup> and electrons (SLAC)<sup>4</sup> is shown in Fig. 4. There is now good agreement between the results with the two probes. In these graphs and in many more throughout the rest of

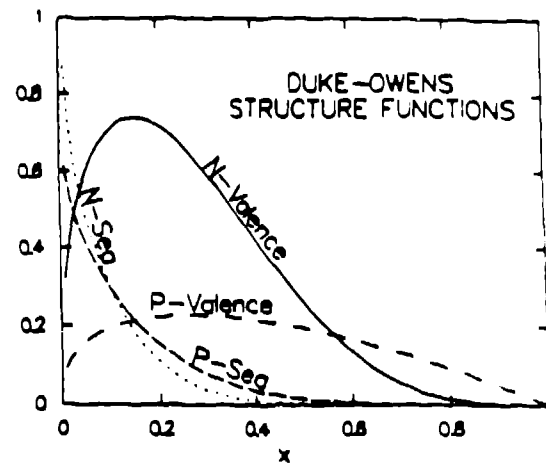


Fig. 2. Nucleon and pion structure functions from Duke, Owens (Ref.<sup>1</sup>).

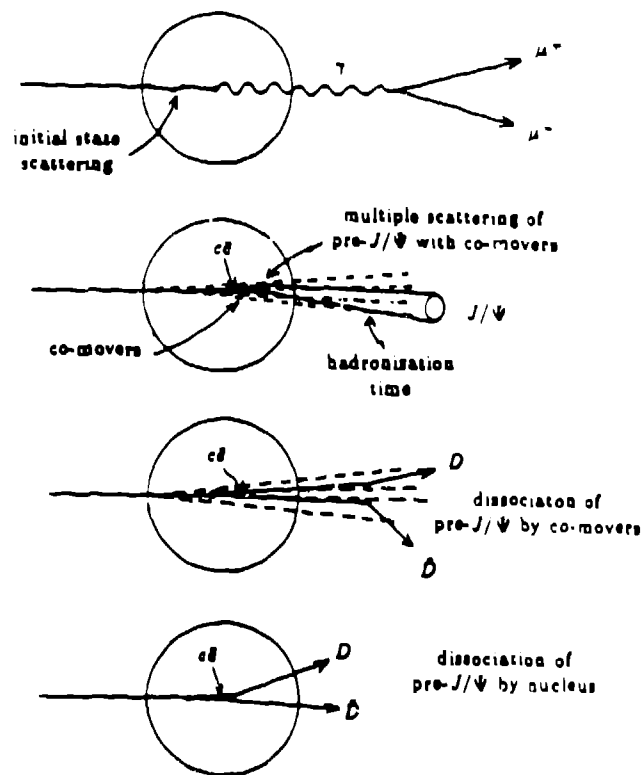


Fig. 3. Some of the reaction dynamics effects for Drell-Yan and  $J/\psi$  production in nuclei.

this talk I will show the ratio of structure functions between a heavy nucleus and deuterium,  $R(A/D)$ , versus target quark momentum fraction,  $x_1$ . If the data points all fell on the horizontal line at  $R = 1$  then there would be no nuclear medium effect. However for the DIS data shown there is a depletion of the low-momentum quarks (shadowing region), no modification just above  $x = 0.1$ , an increasing depletion in the intermediate  $x$  region, and a sharp increase toward enhancement at very large  $x$  (due to Fermi motion). This modification

of the nucleon structure function in nuclei is commonly referred to as the EMC effect after the collaboration that first observed it. Some of the newer EMC results,<sup>5</sup> as shown in Fig. 5, indicate that the onset point of the shadowing region moves to larger  $x$  for heavier nuclei; a feature which must be understood by any successful theory of shadowing. Data is also available from neutrino scattering<sup>6</sup> and is consistent with the DIS results but has rather large uncertainties.

## II. Theoretical Models of the EMC effect

Now I will try to identify the basic physics contained in some of the common theoretical models of the EMC effect. I will do this only in very simple terms and will show schematic graphs of the general features expected in the ratio between heavy and light nuclei,  $R(A/D)$ , versus target quark momentum fraction,  $x_2$ . Real model calculations may give somewhat different results; the behavior shown here is only meant to give the reader some simple insight into these effects.

### 1) Nuclear binding and Fermi motion<sup>7-9</sup>:

In principle nuclear binding will produce excess pions in the nucleus which would carry off some of the nucleon momentum and thus cause a reduction in the apparent momentum fraction of the quarks in the nucleus. This produces an effect in the ratio as shown in Fig. 6a. However the pion has a valence anti-quark (which has a fairly hard momentum fraction - see Fig. 1) while the nucleon has only soft (sea) anti-quarks. Thus the excess pions in a heavy nucleus might be expected to cause an increase of the ratio at large  $x$  for the Drell-Yan process which is

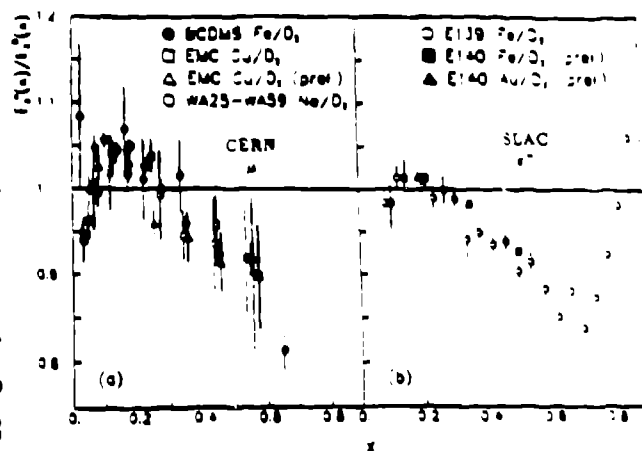


Fig. 4. Deep inelastic scattering data from CERN<sup>3</sup> and SLAC<sup>4</sup>.

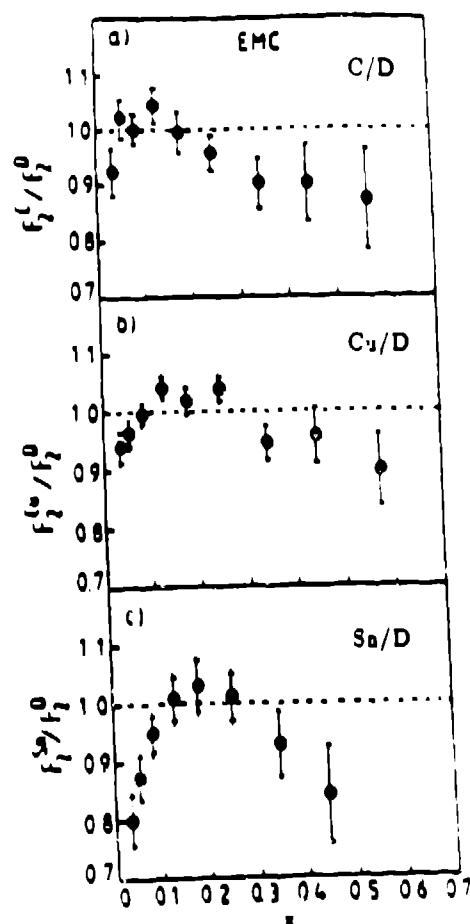


Fig. 5. New EMC results<sup>5</sup> in the shadowing region. Even more recent results which concentrate heavily on the shadowing region can be found in Ref.<sup>26</sup>.

primarily sensitive to the anti-quarks (Fig. 6b).

At large  $x$  the nucleon structure function is very small. However Fermi motion in a nucleus can spread this distribution to produce a finite population near  $x = 1$ . A ratio such as shown in Fig. 6c results.

## ii) Rescaling<sup>10-12</sup>:

The rescaling model in it's simplest form is a phenomenological relationship where the structure function in a nucleus is equal to the unmodified nucleon structure function evaluated at a larger  $Q^2$ , i.e.

$$F_2^{Fe}(x, Q^2) \simeq F_2^D(x, \xi Q^2).$$

With  $\xi \simeq 2$  reasonably good agreement is obtained with the DIS data. This is equivalent to a  $\sim 15\%$  increase in the QCD confinement scale.<sup>12</sup> A larger size scale corresponds to a lower momentum. Thus the momentum fraction of the quarks is softened and there is a loss of valence quark momentum. The resulting dependence of the ratio will then look something like Fig. 6d. One simple model which produces such an increase of scale is that of Close, Jaffee, Roberts, and Ross<sup>12</sup> where they introduce an increased confinement scale that is proportional to the overlap of nucleons. The nucleon overlap is calculated using different correlation functions and single-particle densities. They then assume that when two nucleons overlap their quarks then propagate over a larger spatial domain resulting in a corresponding increase in scale.

## iii) Multi-quark clusters<sup>13-14</sup>:

Multi-quark cluster models obtain a larger length scale by assuming a probability ( $\sim 16 - 30\%$ ) for nucleons in a nucleus to form six or more quark clusters. This should produce the same kind of dependence on  $x$  in the ratio as does rescaling. However, as shown in Fig. 6e, a relative enhancement near  $x = 1$  should also be produced since one quark can assume the momentum of a single nucleon or more.

## iv) Shadowing:

Shadowing refers to the depletion of low-momentum partons (quarks and gluons) in the region of  $x < 0.1$ . Classically the name "shadowing" refers to the phenomena where a nuclear cross section increases with  $A^\alpha$  where  $\alpha$  is less than one. This would occur, e.g. in photon reactions, when the interior

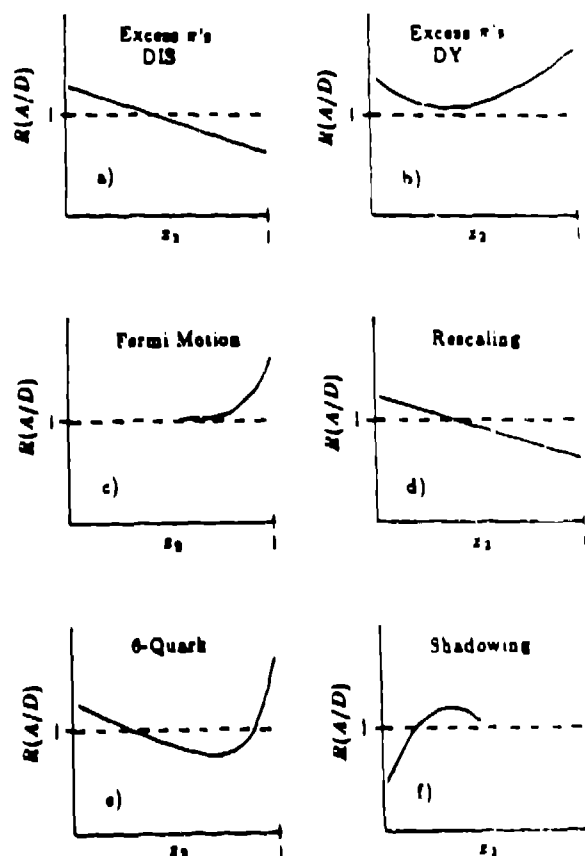


Fig. 6. Schematic expectations for different EMC models as labeled.



of the nucleus was shadowed by a front surface which strongly interacts with the probe or is black. However in the discussion of structure functions the term is used to refer only to the low  $x$  region where the cross section per nucleon decreases faster than  $A$  (i.e.  $\alpha < 1$ ). One simple explanation of this phenomena is that the low- $x$  partons have a large spatial extent and therefore overlap and interact causing a redistribution of their momenta.<sup>15</sup> The typical effect of shadowing on the ratio is shown in Fig. 6f where there is a slight enhancement or "anti-shadowing" just above  $x = 0.1$  in addition to the depletion below  $x = 0.1$ . Another recent explanation of the shadowing phenomena from Brodsky and Lu<sup>16</sup> involves a detailed parton multiple scattering picture and produces similar effects in the ratio.

A set of model calculations from Bickerstaff, Birse, and Miller<sup>8</sup> are shown for DIS and Drell-Yan in Fig. 7. These calculations give fair agreement with the DIS data but give large differences in their prediction for DY. Thus data for the Drell-Yan process is expected to distinguish between the models.

### III. Drell-Yan and E772

Fermilab E772 measures the  $A$ -dependence of the Drell-Yan process at a c.m. energy of  $\sim 39$  GeV by colliding 800 GeV protons with fixed nuclear targets. By measuring the momenta of the muon pair one can then calculate the beam quark and target quark momentum fractions. The differential cross section is related to the structure functions by,

$$\frac{d^2\sigma}{d\Lambda^2 dx} = K(Q^2, x_F) \frac{8\pi\alpha^2}{9M^3} \frac{x_1 x_2}{x_1 + x_2} \sum e_i^2 \{F_i^1(x_1)F_i^2(x_2) + F_i^1(x_1)F_i^2(x_2)\},$$

where  $x_1(x_2)$  is the beam (target) quark momentum fraction and  $F_i^j(F_i^j)$  is the quark (anti-quark) structure function with  $j = 1, 2$  corresponding to beam, target, and where the sum over  $i$  is over types of quarks. The  $K$ -factor in front of this expression represents QCD

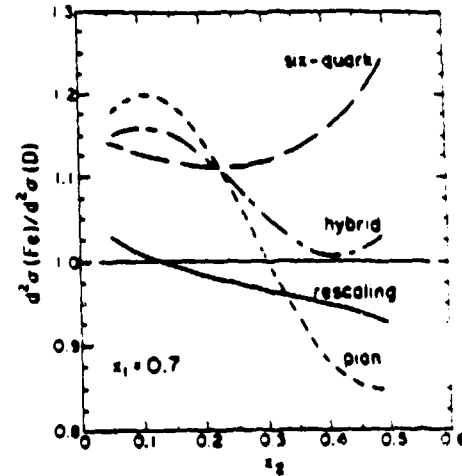
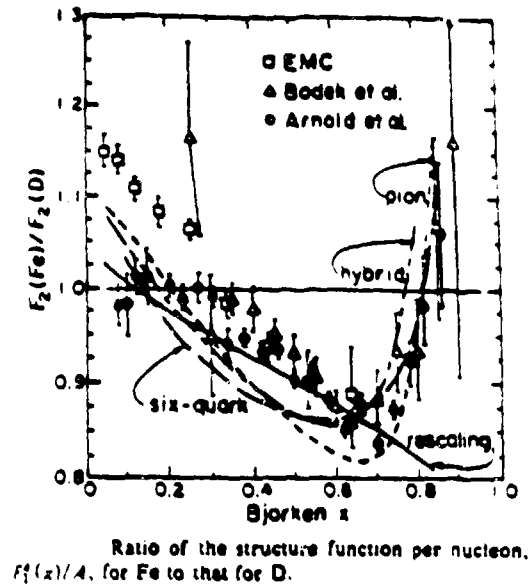


Fig. 7. Calculations of the ratio of the structure function per nucleon for Fe to that of D for deep inelastic scattering and for Drell-Yan from Ref.<sup>8</sup>.

corrections and is  $\sim 2$ ; however the cross-section factorizes<sup>17</sup> so that this factor is constant over the quark momentum fraction. Thus in our experiment, which involves almost exclusively the product of the beam quark and target anti-quark structure functions the cross section is a direct measurement of this structure function product.

The detector used at Fermilab for E772 is shown in Fig. 8. Drell-Yan cross sections in the  $3 \leq M_{\mu^+\mu^-} \leq 16\text{GeV}$  region are only a few  $\text{pb's/GeV}$ . However this detector has good acceptance for  $\mu^+\mu^-$  pairs ( $\approx 5\%$ ) and can handle a very high rate of protons on target (up to  $2 \times 10^{12}/\text{spill}$ ). The portion of the 800 GeV protons which does not interact in the target is absorbed in the beam dump contained within the first magnet. Produced muon pairs are analyzed by two large magnets with a total  $p_T$ -kick of about 6 GeV. A copper/carbon/polyethylene absorber near the rear of the first magnet protects the detectors downstream of the first magnet from low energy particles from the target, beam

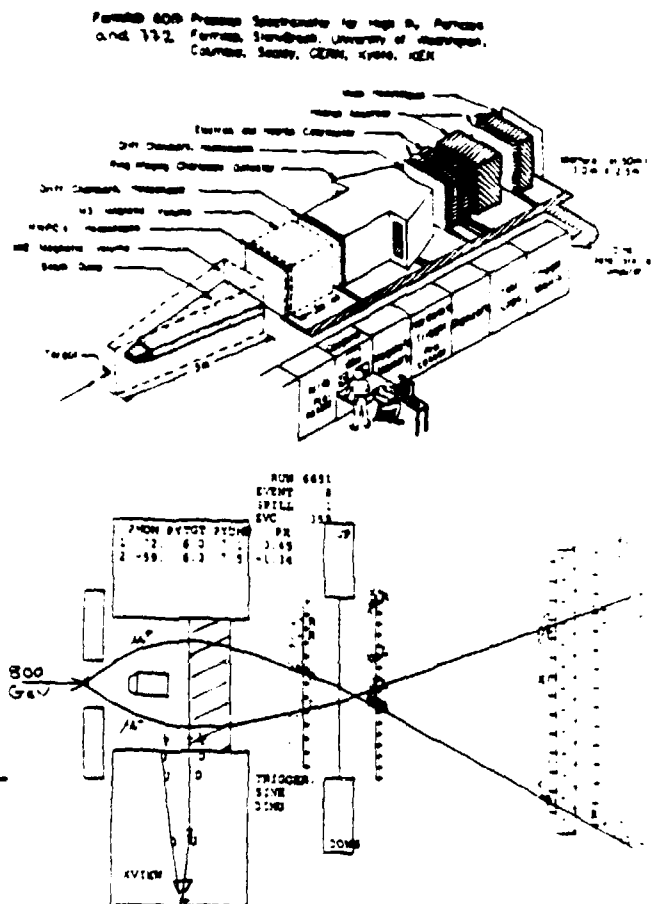


Fig. 8. The Fermilab E605/E772 pair spectrometer with a reconstructed event shown in the bottom panel.

dump, or magnet walls. Several sets of scintillator hodoscopes and wire chamber or drift chamber planes throughout the rest of the detector accurately determine the momenta of the two muons. A calorimeter and a thick absorber assure that only muons penetrate through to the rearmost planes of detectors which then provide a clear muon identification. The measured momenta and the track angles are then used to construct physics quantities. The resulting mass spectra is shown in Fig. 9. In addition to the Drell-Yan continuum we also see the  $J/\psi$  and  $\psi'$  peaks near the lower end of the acceptance and several  $\Upsilon$  peaks near the high end. For the Drell-Yan results that will be shown throughout the rest of this paper only the cross-hatched areas ( $4 < M < 9$  and  $M > 11$  GeV) will be used in order to avoid systematic errors related to peak determination for the resonances. The data obtained for the three settings of the magnets is summarized in Table I. as are the statistical uncertainties for the Drell-Yan data obtained for the different  $x_2$  bins covered by the experiment. Of the 670k total dimuon events there are 450k Drell-Yan pairs, 100k  $J/\psi$ 's, 12k  $\psi'$ 's, and 27k  $\Upsilon$ 's. Careful and redundant beam monitoring, target thickness determinations, and frequent target interchange resulted in a total systematic error of less

TABLE I - E772 DATA SUMMARY

Magnet Setting	$\langle M(\mu^+\mu^-) \rangle$	Targets	Proton Flux	Dimuon Events
Low mass	4.8 GeV	$Fe/Ca/LD_1$	$6 \times 10^{15}$	170 k
		$W/C/LD_1$	$2 \times 10^{15}$	70 k
Medium mass	6.5 GeV	$Fe/Ca/LD_1$	$2.4 \times 10^{16}$	280 k
		$W/C/LD_1$	$0.9 \times 10^{16}$	110 k
High mass	9.1 GeV	$Fe/Ca/LD_1$	$1.5 \times 10^{16}$	40 k
TOTAL			$5.6 \times 10^{16}$	670 k

Statistical Errors in Drell-Yan Cross Section Ratios for Various  $x_2$  Bins ( $x_F > 0$ )

Target	0 - 0.05	0.05 - 0.1	0.1 - 0.15	0.15 - 0.2	0.2 - 0.25	0.25 - 0.3
Ca,Fe	1%	< 1%	1%	2%	5%	12%
C,W	2%	1%	2%	4%	10%	24%

than 2%. Our Drell-Yan results will shortly be published in a Physical Review Letter.<sup>18</sup> However the resonance results that will be shown below are still preliminary.

#### A-dependence of Drell-Yan

The Drell-Yan results in terms of the ratio between heavy and light target versus  $x_1$  ( $x_2$ ) are shown in Fig. 10. If there were no modification of the nucleon anti-quark structure function by the nuclear medium the data would fall on a ratio of one. In fact the data is consistent with one except in the low- $x$  shadowing region where a significant depletion can be seen as the nuclear mass gets large (i.e. for  $W/{}^2H$ ). We have plotted the EMC results<sup>3</sup> for  $Sn/{}^2H$  with our  $W/{}^2H$  results in the bottom right panel. The depletion in the shadowing region for the EMC data is significantly stronger than that seen in our data suggesting that the anti-quarks are not depleted as strongly as are the valence quarks. For our  $Fe/{}^2H$  ratio we compare with specific model calculations obtained from Hwang, Moss, and Peng.<sup>19</sup> The pion excess model uses a  $g'_0 = 0.6$  and badly misses the data. The quark cluster calculation which follows the model of Carlson and Havens<sup>13</sup> and uses a 6-quark cluster probability of 15% also badly misses the data. Only the rescaling model agrees well with the data. The disagreement for  $x \leq 0.1$  can presumably be fixed by adding in a depletion due to shadowing.

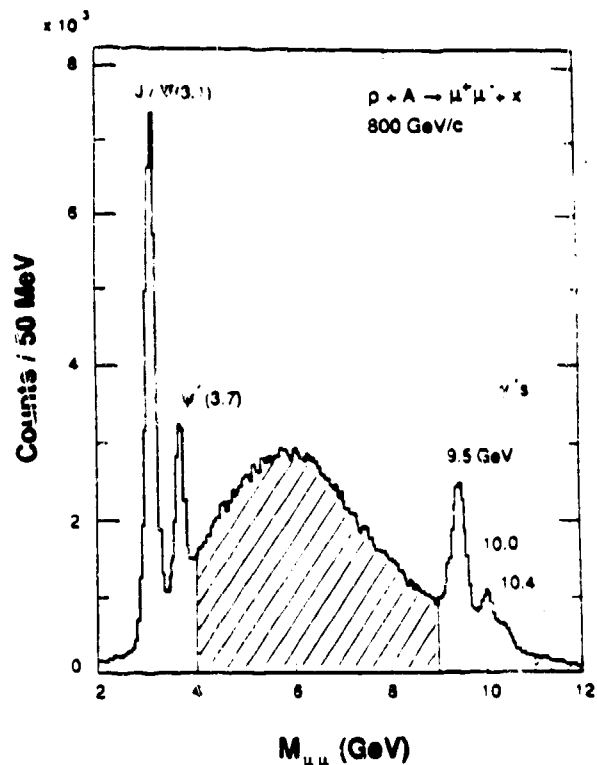


Fig. 9. Muon-pair mass spectra obtained in E772 for 800 GeV protons on deuterium.

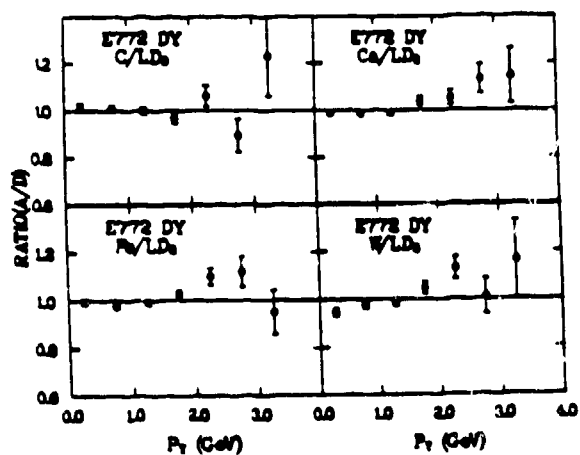


Fig. 11.  $p_T$ -dependence of the Drell-Yan ratio.

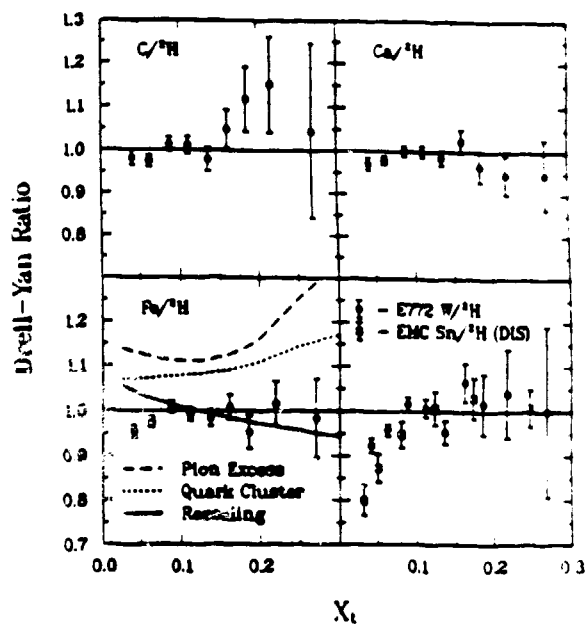


Fig. 10. Target momentum fraction ( $x_t$ ) dependence of the Drell-Yan dimuon yield per nucleon for positive  $x_F$ . The curves shown for  $Fe/^2H$  are predictions of various models as described in the text. Also shown are the deep inelastic scattering data for  $Sn/^2H$  from the EMC.<sup>3</sup>

$$NA10 \quad \frac{\sigma(\pi^- W \rightarrow \mu^+ \mu^- + X)}{\sigma(\pi^- D \rightarrow \mu^+ \mu^- + X)}$$

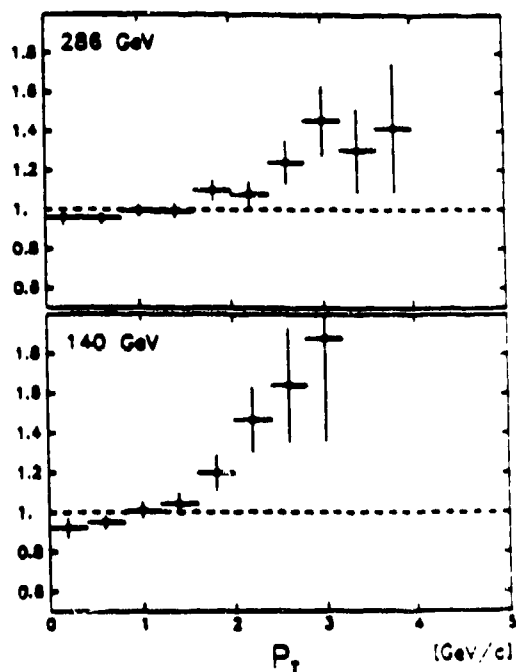


Fig. 12.  $p_T$ -dependence of the pion-induced Drell-Yan ratio from NA10.<sup>2</sup>

Our results for the  $p_T$  dependence of the Drell-Yan ratio are shown in Fig. 11. An increase in  $p_T$  with mass can be seen, consistent with expectations based on initial-state multiple scattering. A similar effect, shown in Fig. 12, was seen in pion-induced Drell-Yan (NA10).<sup>20</sup> The effect at 140 GeV is substantially larger than seen in E772 but at 286 GeV their pion data is consistent with our proton data.

### A-dependence of Resonance Production

The mass dependence of the ratio of total cross sections for resonance production from E772 is shown in Fig. 13. Also shown for comparison is the Drell-Yan data whose total cross section has no mass dependence and lies on the horizontal line at  $R = 1$ . The E772 resonance results are *preliminary*; a more careful determination of the peak shapes and yields is in progress. All the resonances shown have a strong A-dependence with the lighter resonances ( $J/\psi$  and  $\psi'$ ) having the strongest suppression with mass. A simple fit of the form  $R = A^\alpha$  has been done to the resonances (with the  $J/\psi$  and  $\psi'$  fit together). The resulting  $\alpha$ 's are 0.963 for the  $\Upsilon$  and 0.916 for the  $J/\psi$  and  $\psi'$ . Although some of this anomalous A dependence could be caused by a modification of the gluon structure function in nuclei it seems likely that most of it caused by nuclear effects in the final-state such as those described in Section I. Some recent data from WA82 for  $D$ -meson production suggests that the A-dependence for  $D$ 's may be even stronger than that for the  $J/\psi$ .<sup>21</sup>

The  $p_T$  dependence of the  $J/\psi$  ratio is shown in Fig. 14. One can see the same increasing ratio at large  $p_T$  that was seen for the Drell-Yan process, again presumably due to multiple scattering. Another striking feature of the data is shown in Fig. 15 where we plot the mass dependence of the ratio

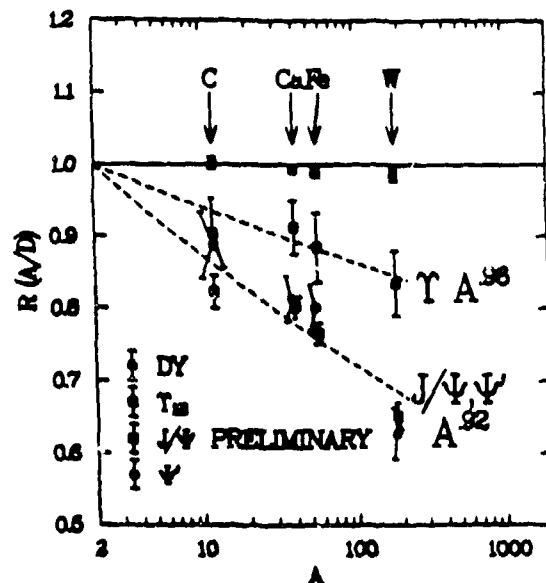


Fig. 13. Preliminary nuclear-mass dependence of resonance production compared to Drell-Yan for the ratio from E772. For the  $\Upsilon$  and for the  $J/\psi + \psi'$  results of  $A^\alpha$  fits are shown.

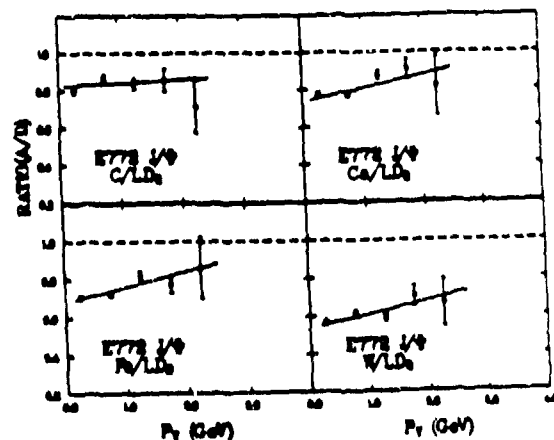


Fig. 14. Preliminary  $p_T$ -dependence for  $J/\psi$  production from E772. (The curves are to guide the eye).

for different ranges of  $x_F$  where  $x_F = x_1 - x_2$  and essentially is a measure the longitudinal momentum of the resonance. Again fits to the form  $R = A^\alpha$  have been made for each bin in  $x_F$  and show that the attenuation of the  $J/\psi$ 's is much stronger for large  $x_F$ .

Where does this  $x_F$  dependence come from? Fig. 16 shows  $\alpha$  as a function of target momentum fraction,  $x_2$ , for our  $J/\psi$  results and for those from NA3<sup>22</sup> which studied  $J/\psi$  suppression at a lower energy. The reduction of  $\alpha$  below  $\sim 0.9$  begins at a much higher  $x_2$  for the lower energy data. It seems clear that the bulk of this suppression does not reflect a change in the intrinsic nucleon gluonic-structure. However a comparison of the  $x_F$  dependence of the two experiments, Fig. 17, shows that they have essentially the same  $x_F$  dependence. Could some of the observed effect be caused by a shift in the  $x_F$  distribution as shown in Fig. 18? In order to answer this question more data at and below  $x_F = 0$  is required. In our next experiment at Fermilab, E789, we will extend the kinematic range of our  $J/\psi$  measurements to address this question. We also plan to try to make A-dependence measurements of the production of  $D$ 's via their two-body decay to  $\pi K$ .

$J/\psi$  suppression has also been observed in heavy-ion collisions. Yields of  $J/\psi$  relative to the Drell-Yan background are reduced in central collisions relative to peripheral collisions, as shown in Fig. 19. Central collisions, which correspond to small impact parameter, are presumed to be able to create quark-gluon plasma for which such a suppression was predicted.<sup>23</sup> However it is clear that whatever effects are responsible

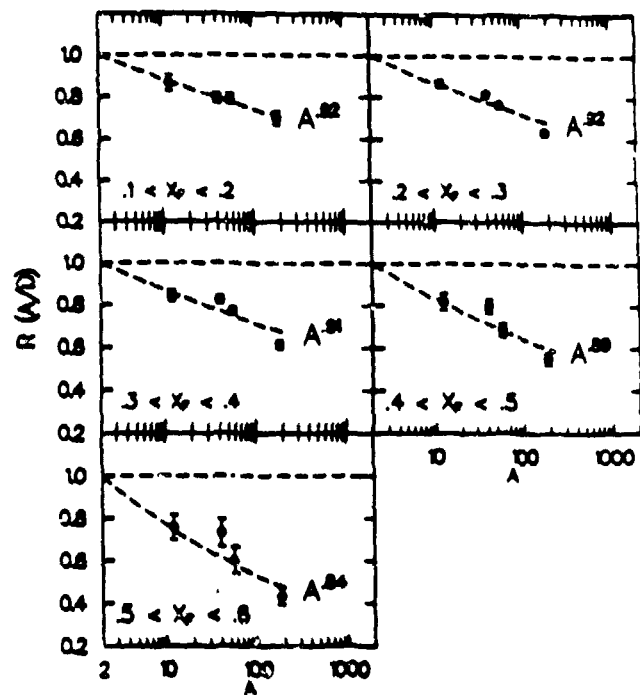


Fig. 15. Preliminary mass-dependence from E772 of the ratio for  $J/\psi$  production for different ranges in  $x_F$ .

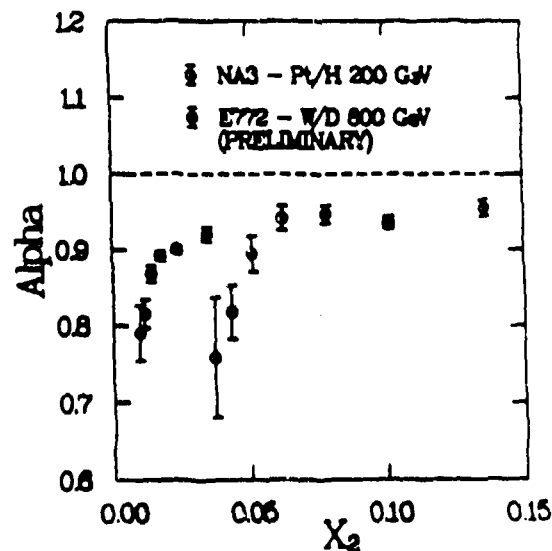


Fig. 16.  $x_2$ -dependence of  $\alpha$  (from fits of the mass dependence to  $A^\alpha$ ) versus  $x_2$  from NA3 and E772 (preliminary).

for the suppression of proton-nucleus  $J/\psi$  production may also play an important role in heavy-ion  $J/\psi$  production and could explain most of the suppression seen with heavy-ions.

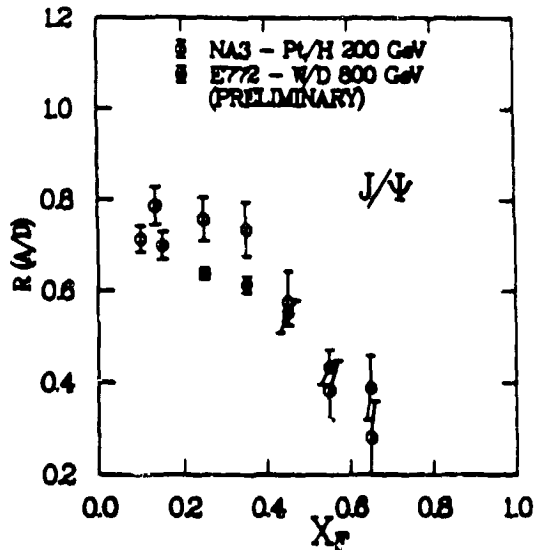


Fig. 17.  $x_F$ -dependence of  $\alpha$  (from fits of the mass dependence to  $A^\alpha$ ) versus  $x_F$  from NA3 and E772 (preliminary).

### Conclusions

Precise measurements of the  $A$ -dependence of the Drell-Yan and of resonance ( $J/\psi$ ,  $\psi'$ ,  $\Upsilon$ ) production have been made in Fermilab E772. The anti-quark structure function is not affected by the nuclear medium up to  $x \leq 0.3$  except in the shadowing region at very small  $x$  ( $x \leq 0.1$ ). Models which produce a significant anti-quark enhancement or depletion for  $0.1 \leq x \leq 0.3$  are ruled out.

The  $p_T$  distribution is broadened, presumably due to initial-state effects. Resonance production is clearly suppressed in nuclei. It is not clear how to decouple structure and reaction mechanism effects in order to extract the  $A$ -dependence of gluon structure functions.  $J/\psi$  suppression in proton-nucleus and in heavy-ion collisions probably share common physical origins (e.g. final-state effects). Thus the latter is unlikely to be a good indicator for quark-gluon plasma.

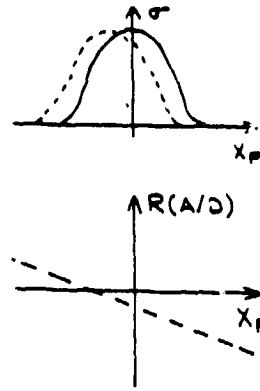


Fig. 18. Cartoon picture of how a shift in the  $x_F$  distribution affects the ratio.

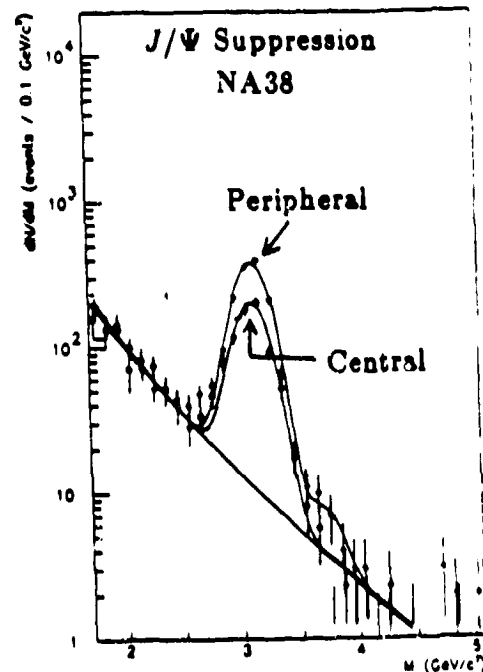


Fig. 19. The suppression of  $J/\psi$  production in central relative to peripheral heavy-ion collisions.

## References

- <sup>1</sup>D. W. Duke and J. F. Owens, Phys. Rev. D30 (1984) 49.
- <sup>2</sup>S. Gavin and R. Vogt, preprint, LBL-27417 (1989).
- <sup>3</sup>J. J. Aubert, *et al.*, Phys. Lett. B123 (1983) 275 .
- <sup>4</sup>Proceedings of the 1987 International Symposium on Lepton and Photon Interactions at High Energies, Hamburg, 27-31 July, 1987; edited by W. Bartel and R. Ruckl, North-Holland, Amsterdam.
- <sup>5</sup>J. Ashman, *et al.*, Phys. Lett. B202 (1988) 603.
- <sup>6</sup>J. G. H. de Groot, *et al.*, Z. Physik C1 (1979) 143.
- <sup>7</sup>M. Ericson and A. W. Thomas, Phys. Lett. 128B (1983) 112.
- <sup>8</sup>R. P. Bickerstaff, M. C. Birse, and G. A. Miller, Phys. Rev. Lett. 53 (1984) 2532.
- <sup>9</sup>E. L. Berger, F. Coester, and R. B. Wiringa, Phys. Rev. D29 (1984) 398.
- <sup>10</sup>F. E. Close, R. G. Roberts, and G. G. Ross, Phys. Lett. 129B (1983) 346.
- <sup>11</sup>R. L. Jaffee, Phys. Rev. Lett. 50 (1983) 228.
- <sup>12</sup>F. E. Close, R. L. Jaffee, R. G. Roberts, and G. G. Ross, Phys. Rev. D31 (1985) 1004.
- <sup>13</sup>C. E. Carlson and T. J. Havens, Phys. Rev. Lett. 51 (1983) 261.
- <sup>14</sup>Hans J. Pirner and James P. Vary, Phys. Rev. Lett. 46 (1981) 1376.
- <sup>15</sup>N. N. Nicolaev and V. I. Zakharov, Phys. Lett. B55 (1975) 397; A. H. Mueller and J. Qiu, Nucl. Phys. B268 (1986) 427; and Edmond L. Berger and Jianwei Qiu, Phys. Lett. B141 (1988) 119.
- <sup>16</sup>Stanley J. Brodsky and Hung Jung Lu, Phys. Rev. Lett. 64 (1990) 1342.
- <sup>17</sup>G. Altarelli, R. K. Ellis, and G. Martinelli, Nucl. Phys. B157 (1979) 461; J. C. Collins, D. E. Soper, and G. Sterman, Phys. Lett. 134B (1984) 263; and I. R. Kenyon, Rep. Prog. Phys. 45 (1982) 1261.
- <sup>18</sup>D. M. Alde, *et al.*, Phys. Rev. Lett. 21 (1990) 2479.
- <sup>19</sup>W. Y. P. Hwang, J. M. Moss, and J. C. Peng, Phys. Rev. D38 (1988) 2785.
- <sup>20</sup>P. Bordalo, *et al.*, Phys. Lett. B193 (1987) 373.
- <sup>21</sup>A. Forino, *et al.* (WA82) preprint.



<sup>22</sup>J. Badier, *et al.*, *Z. Phys.* C20 (1983) 101.

<sup>23</sup>T. Matsui and H. Satz, *Phys. Lett.* B178 (1986) 416.

<sup>24</sup>C. Baglin, *et al.*, *Phys. Lett.* B220 (1989) 471.

<sup>25</sup>M. Arneodo, *et al.*, *Phys. Lett.* B211 (1988) 493.